Publication I

Tero Kiuru, Ville S. Möttönen, and Antti V. Räisänen. 2007. *W*-band waveguide impedance tuner utilizing dielectric-based backshorts. IEEE Transactions on Microwave Theory and Techniques, volume 55, number 8, pages 1659-1665.

W-Band Waveguide Impedance Tuner Utilizing Dielectric-Based Backshorts

Tero Kiuru, *Student Member, IEEE*, Ville S. Möttönen, *Member, IEEE*, and Antti V. Räisänen, *Fellow, IEEE*

***Abstract*—We present the design, simulations, fabrication, and measurements of a W-band waveguide impedance tuner. The design consists of a WR-10 waveguide with two E-plane arms for tunable dielectric-based backshorts. The impedance tuner is fabricated using a simple split-block technique and is easily scalable to submillimeter wavelengths. Our design shows an excellent input impedance range, tuning accuracy, repeatability, and a high attainable maximum reflection coefficient over the frequency band of 75–110 GHz. Our tuner applies dielectric-based backshorts, which provide a tuning accuracy better than that of other waveguide backshorts.**

***Index Terms*—Dielectric-based backshort, impedance tuner, E-plane, waveguide, W-band.**

I. Introduction

AT MILLIMETER and submillimeter wavelengths, the input and output powers of devices are usually low. Consequently, accurate and reliable source and load impedance determination is important, e.g., in a mixer or multiplier optimization and in a low-noise amplifier (LNA) design. In addition, an accurate and reliable reflection coefficient setting is important for noise parameter measurements at microwave and millimeter-wave regions [1]–[3]. For example, at least four noise-figure measurements with different source reflection coefficients have to be made in order to determine the noise parameters of a linear two-port. The noise figure is then extracted with mathematical fitting methods [2]. The accuracy of the calculated noise parameters depends on the accuracy of the source reflection coefficients.

An impedance tuner is a key element in a source or load impedance determination. Commercially, wideband waveguide impedance tuners are available up to 170 GHz. One operating principle of these tuners is based on a needle probe inserted inside the waveguide. The place and depth of the probe determines the phase and magnitude of the reflection coefficient [4], [5].[1] A design with a waveguide magic-T using tuning arms is commercially available[2] and impedance tuners employing traditional waveguide backshorts as tuning elements have been in use for some time, e.g., in klystron matching [6] and in noise parameter measurements [7]. The performance of these designs at submillimeter wavelengths degrades due to the complex structures and scaling difficulties of the traditional backshorts. A waveguide transition in [8] applies for the impedance tuning a new low-loss noncontacting waveguide backshort. Both the measured performance at the V-band and simulated performance at 1.6 THz are good. However, according to measurements and simulations, this design is prone to resonances.

Recently, research on the impedance tuners based on microelectromechanical systems (MEMS) has been vigorous, e.g., [9]–[11]. MEMS-based tuners are compact and electrically tunable. However, at higher millimeter-wave frequencies, the maximum attainable reflection coefficient of MEMS-based backshorts is less than that of the waveguide backshorts, and, to the best of the authors' knowledge, electrically tunable MEMS-based backshorts have not been demonstrated at submillimeter wavelengths. Reference [12] describes a micromechanical tuning element, called a sliding planar backshort, which can be fabricated with photolithographic micromachining techniques. Tests in a coplanar waveguide environment indicate an excellent return loss at 620 GHz. The mechanical tuning of this backshort is very challenging.

In this paper, we present the design, simulations, fabrication, and measurements of a novel waveguide impedance tuner for the W-band (75–110 GHz). The waveguide impedance tuner consists of a main waveguide (WR-10) and E-plane arms (WR-10) with dielectric-based backshorts. This tuner shows an excellent impedance range, tuning accuracy, repeatability, and a high attainable maximum reflection coefficient [high voltage standing-wave ratio (VSWR)] over the entire W-band. Moreover, our design is easily scalable up to submillimeter wavelengths.

II. Design of Waveguide Impedance Tuner

A. Basic Structure

We use two series, i.e., E-plane, tuning elements in our W-band (frequency range: 75–110 GHz) waveguide impedance tuner. The tuner has WR-10 waveguides with the width $a = 2.54$ mm and height $b = 1.27$ mm. The use of series tuning elements enables easier fabrication and assembly in the case of split-waveguide block techniques. Two elements provide a very large impedance range and, in addition, the tuner structure does

Manuscript received November 30, 2006; revised March 23, 2007. This work was supported in part by the Academy of Finland and Tekes–Finnish Founding Agency for Technology and Innovation under the Centre of Excellence Program.

T. Kiuru and A. V. Räisänen are with the TKK Helsinki University of Technology, SMARAD Centre of Excellence/Radio Laboratory, Millimetre Wave Laboratory of Finland (MilliLab), Espoo FI-02015 TKK, Finland (e-mail: tero.kiuru@tkk.fi).

V. S. Möttönen was with the TKK Helsinki University of Technology, SMARAD Centre of Excellence/Radio Laboratory, Millimetre Wave Laboratory of Finland (MilliLab), Espoo FI-02015 TKK, Finland. He is now with the National Board of Patents and Registration of Finland, FI-00101 Helsinki, Finland.

Digital Object Identifier 10.1109/TMTT.2007.901112

[1]Maury Microwave, Ontario, CA. Device characterization, electro-mechanical tuners (ATS), automated tuners. [Online]. Available: http://www.maurymw.com/

[2]Millitech Inc., Northampton, MA. [Online]. Available: http://www.millitech.com/pdfs/specsheets/IS000060-EHT-HBT.pdf

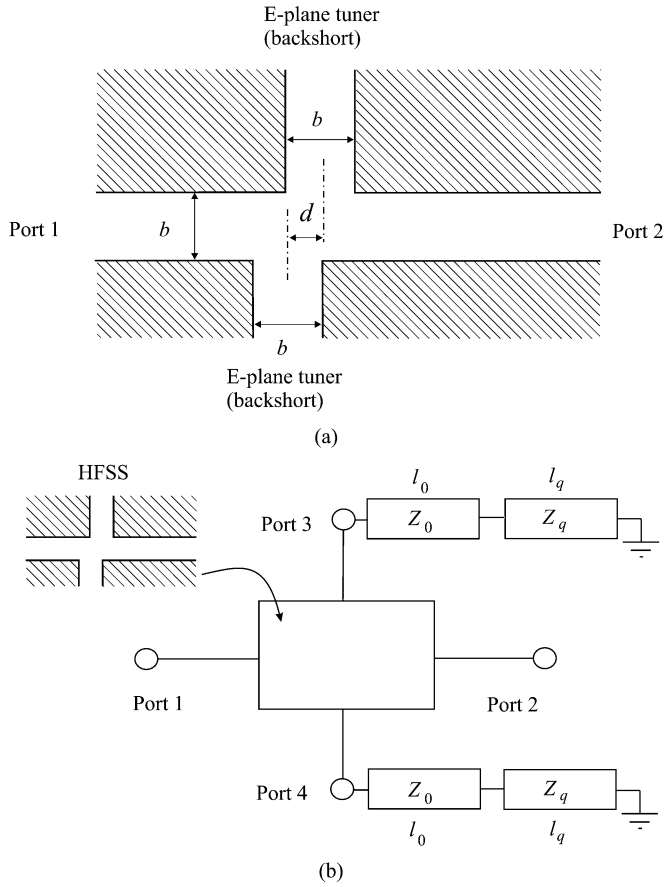

Fig. 1. (a) E-plane T-junctions of the waveguide impedance tuner with equal height waveguides. (b) Equivalent circuit of the tuner in a circuit simulator ADS. Impedances Z_0 and Z_q correspond to the characteristic impedances of an empty waveguide and a waveguide with quartz slab, respectively. Lengths l_0 and l_q correspond to the lengths of these waveguides, respectively. Total length $l_0 + l_q$ is constant. The S-parameter matrix of the double-T junction simulated in HFSS is imported into ADS.

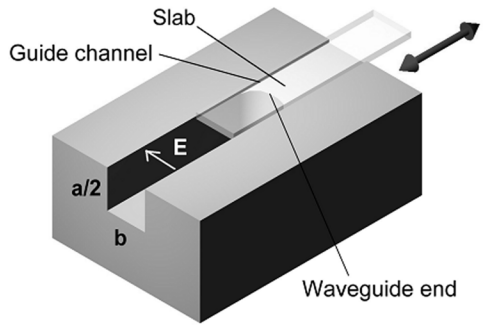

Fig. 2. Dielectric-based tunable waveguide backshort. One waveguide block half is shown with a waveguide end, guide channel, and a dielectric slab. [14].

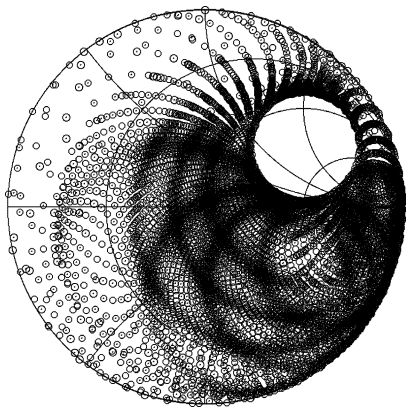

Fig. 3. Simulated input impedance coverage of the lossless tuner on the Smith diagram at 92.5 GHz. The impedance spots correspond to backshort positions with 100-μm steps.

TABLE I
DIMENSIONS AND PARAMETERS OF THE TUNER

MAIN WAVEGUIDE	a	2.54 mm
	b	1.27 mm
	length	35 mm
TUNER E-PLANE ARMS	a	2.54 mm
	b	1.27 mm
	length	13.5 mm
QUARTZ GUIDE CHANNEL	width	1.27 mm
	heigth	200 μm
	length	2.0 mm
DOUBLE-T JUNCTION	d (designed)	500 μm
	d (realized)	470 μm
QUARTZ SLAB	width	1.2 mm
	thickness	127 μm
	ϵ_r	3.8

not become complex. The tuning elements are formed by a tunable backshort [13], [14] in the E-plane arm of the T-junction of equal height waveguides. Fig. 1(a) shows a simplified tuner structure. Different equivalent circuits exist for the waveguide T-junction depending on the T-junction reference planes, e.g., [15, pp. 336–350]. An equivalent circuit can be applied in a circuit simulator for the tuner design. However, we have used a finite-element method-based electromagnetic structure simulator [Ansoft's High Frequency Structure Simulator (HFSS)] to obtain an accurate model for the double-T junction. This model, embedded in a circuit simulator [Agilent's Advanced Design System (ADS)] [see Fig. 1(b)] provides a better design accuracy.

B. Dielectric-Based Backshort as a Tuning Element

Our waveguide tuner uses a dielectric-based backshort [13], [14] as a tuning element. Fig. 2 shows an overview of the backshort. Basically, a dielectric slab, moved inside the waveguide through a hole in a fixed waveguide end, changes the effective electrical length of the structure and, thus, the phase of the reflected wave. A rigid slab aligns well with the guide channel and does not require guide grooves in the waveguide. We have used a 127-μm-thick and 1.2-mm-wide quartz slab (dielectric constant $\epsilon_r = 3.8$) in a 200-μm-high and 1.27-mm-wide guide channel. In [13], we have described the structure, design, and testing of a W-band backshort, and have also compiled the design features. The measured return loss for the W-band backshort with a quartz slab is less than 0.21 dB $(\mathrm{VSWR} > 82)$. Reference [14] studies the effects of different dielectric materials, material thicknesses, a material tapering, and frequency scaling on the backshort performance. In comparison to other existing waveguide backshorts [8], [16]–[26], the one presented here has several important advantages: a simple design and fabrication, easy tuning (physical tuning range greater than with other

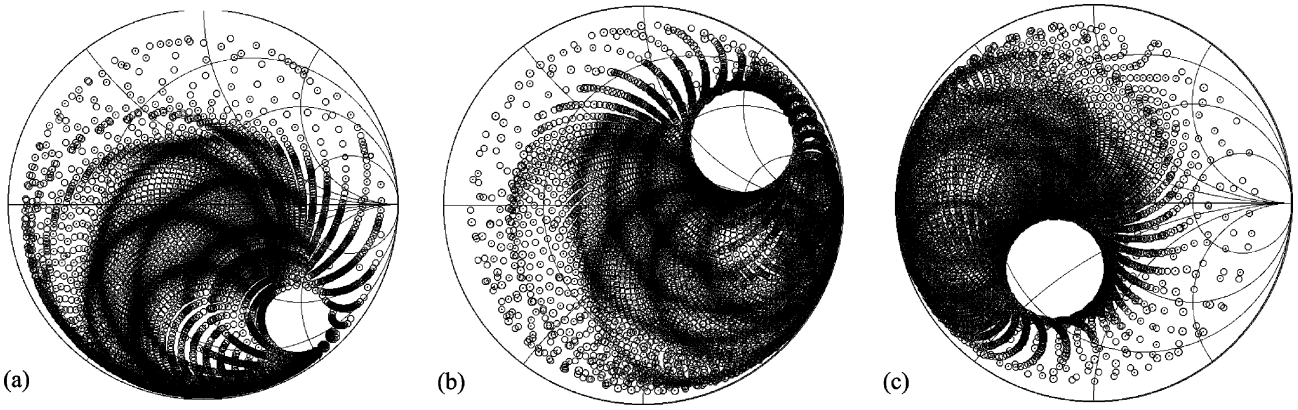

Fig. 4. Simulated input impedance coverage on the Smith diagram when losses are taken into account. (a) 75 GHz. (b) 92.5 GHz. (c) 110 GHz. The impedance spots correspond to backshort positions with 100-μm steps.

backshorts), the most accurate adjustment, low losses, high reliability, insensitivity to alignment errors, not prone to resonances in the operational frequency band like noncontacting backshorts, and readiness for scaling. Features of different backshort designs are further discussed in [14] and [27].

C. Spacing of Tuning Elements

Theoretically, two tuning elements enable matching of almost all the impedances when the spacing d between the elements is close to zero or of the half-wavelength in the waveguide $\lambda_g/2$. However, the tuning is then very sensitive to the frequency. Since λ_g at 75 GHz is twice λ_g at 110 GHz, d has to have an appropriate value in order for the tuner to operate well over the full waveguide frequency band. Since the E-plane arms of the T-junctions are close to each other, we have simulated the double-T junction as one four-port structure in HFSS, and then studied the impedance coverage in ADS with an imported four-port S-parameter matrix and ideal tunable backshorts [see Fig. 1(b)]. By changing d, we have optimized the operation over the W-band. At this point, when optimizing the impedance coverage, we have used lossless structures. The optimization resulted in $d = 500$ mm ($\lambda_g/13$–$2\lambda_g/13$, 75–110 GHz). Fig. 3 shows the simulated input impedance at Port 1 (load impedance in Port 2 is equal to Z_0) (see Fig. 1) for the lossless tuner with 100-μm backshort position steps at 92.5 GHz. The Smith diagram coverage is 96% at 75 GHz, 92% at 92.5 GHz, and 93% at 110 GHz. Table I shows the main dimensions and parameters of the tuner.

D. Effect of Losses

Losses of the waveguide impedance tuner comprise the conductive losses of the waveguide walls and dielectric losses of the quartz slabs. Due to the losses, it is impossible to obtain reflection coefficients with magnitudes very close to unity and, therefore, the Smith diagram coverage is receded from the edges of the diagram. Fig. 4 illustrates the simulated input impedance for the lossy tuner structure with 100-μm backshort position steps. At 75 GHz, the Smith diagram coverage is 81%, 77% at 92.5 GHz and 74% at 110 GHz. By choosing output waveguides of different lengths on each side of the double-T junction, we can change the position of the unmatched region on the Smith diagram by turning the tuner around. This will further increase the achievable Smith diagram coverage. In our design, the length difference between the input and output waveguides is 770 μm, corresponding to a 130° phase difference in the reflection coefficient at 92.5 GHz if the tuner is turned around. The simulated combined Smith diagram coverage from Port 1 and Port 2 is 91% at 75 GHz, 94% at 92.5 GHz, and 94% at 110 GHz. The already low losses of our design can be further reduced by decreasing the length of the waveguides. Measurements and simulations show that the minimum length where the tuning elements still provide a phase shift of 360° over the entire W-band is 10.6 mm. Therefore, the tuning element waveguides could be 1.9 mm shorter. The length of the main waveguide in our design is 35 mm. Theoretically, only the correct function of the double-T junction limits the main waveguide length. This limit is only a few millimeters at the W-band. In reality, however, the limit is set by the size of the micrometers used for tuning and the space required for the attachment of the waveguide block halves. Dielectric losses could be reduced by using a material with lower losses. Suitable materials are unfortunately scarce. We use fused quartz due to its rigidity, low loss, and isotropic permittivity.

III. Fabrication and Assembly

Fig. 5 shows the fabricated tuner. The dielectric slab moves inside the waveguide through the guide channel. The slab is fixed by pressure to a slide, which has a grooved shape to reduce friction. A magnet placed in the other end of the slide connects the slide to the micrometer head with a nonrotating spindle. By using the magnet, misalignment in the micrometer fastening does not affect the slab alignment. The metal elements of the tuner are made of aluminium alloy using the split-block technique and the dielectric slabs are made of fused quartz. The following fabrication and assembly steps are taken.

Step 1) *Waveguide Milling:* The slide channels and the WR-10 main waveguide together with the waveguides for the tuning elements are milled using the split-block technique. After milling, the split-waveguide block halves are gold-coated for optimal electrical operation.

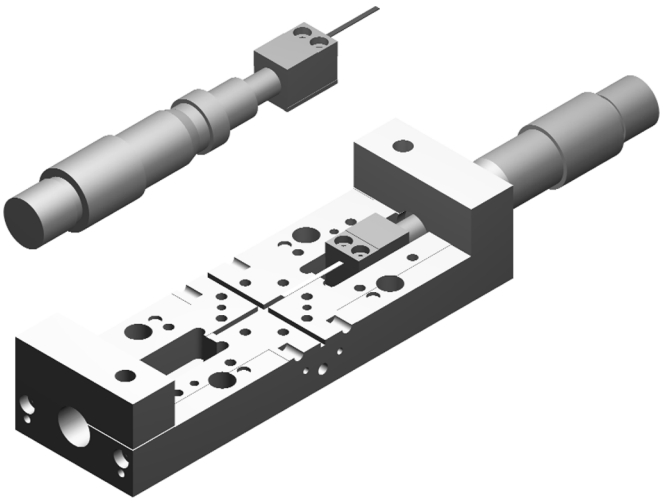

Fig. 5. Waveguide impedance tuner with one split-waveguide block half removed. One micrometer head with a slide and dielectric slab is shown separately.

Step 2) *Fabrication of the Slides:* The slides for the dielectric slabs are milled to the required size and shaped to minimize the friction. Strong permanent magnets are embedded in the slides for the attachment of the slides to micrometer spindles.

Step 3) *Milling of the Guide Channels for the Dielectric Slabs:* The slides are fixed to one split-waveguide block half for the maximum alignment precision of the dielectric slabs. The guide channels are milled simultaneously to the split-waveguide block half and to slides.

Step 4) *Attaching the Dielectric Slabs to the Slides:* The dielectric slabs are positioned in the center of the guide channel so that part of the slab rests on the slide and part on the split-waveguide block half. A pressure piece is attached to the slide in order to clamp the dielectric slab in place.

Step 5) *Assembly of the Impedance Tuner:* After the dielectric slabs and micrometer heads are connected to the slides and the slides are mounted in one of the split-waveguide block halves, the other waveguide block half is installed on top of the first.

IV. Tuner Performance

A. Scattering-Parameter Measurements

The scattering parameters of the waveguide impedance tuner were measured with an HP-8510 vector network analyzer. The frequency range of the measurements was 75–114 GHz and the number of frequency points was 101. The averaging factor was 64. The measured input impedances are shown in Fig. 6 at 75, 92.5, and 110 GHz. The results were obtained by keeping one dielectric slab in place at the end of the waveguide and by moving the other slab in 2-mm steps from the 0 mm (dielectric slab completely drawn in the guide channel) to the 12-mm position. The first slab was then moved 2 mm inside the waveguide. The same procedure was repeated until the both slabs were 12 mm inside the waveguides. Some additional measurements were made in order to better illustrate the impedance coverage on the Smith diagram. The circles in Fig. 6 correspond to the obtainable reflection coefficients with one of the dielectric slabs fixed in place. They are obtained by fitting an equation of a circle using three data points. As a result of fitting with three data points and the fact that the magnitude of the reflection coefficient from the dielectric-based backshort changes slightly as a function of the position of the dielectric slab [13], some measured data points do not lie exactly on the circle. In the simulations of the impedance tuner, the steps for the dielectric slab positions were 100 μm apart. This means that the number of obtained reflection coefficients in the simulations (Figs. 3 and 4) is 400 times greater than in the performed measurements. This, however, is not the limit even for the manually tunable impedance tuner. A careful measurer can easily move the dielectric slabs with 10-μm steps by turning the micrometer heads. With this modest tuning accuracy, the number of obtainable reflection coefficients is 40 000 times greater than that demonstrated here (Fig. 6). With the help of commercial automated linear motors, the achievable step size is in the order of 0.1 μm [4]. This indicates that with a programmable waveguide impedance tuner, virtually any reflection coefficient inside the achievable range could be obtained with outstanding accuracy. The impedance coverage on the Smith diagram calculated from measured data is 70% at 75 GHz, 76% at 92.5 GHz, and 71% at 110 GHz. The maximum attainable reflection coefficient is 0.935 (VSWR $= 29.8$) at 75 GHz, 0.96 (VSWR $= 49$) at 92.5 GHz, and 0.952 (VSWR $= 40.7$) at 110 GHz. Table II comprises the results of the tuner measurements. The achieved Smith diagram coverage correlates well with the simulations at 92.5 GHz (77%) and at 110 GHz (74%) and moderately well with that at 75 GHz (81%). According to simulations, the Smith diagram coverage is very sensitive to the tuning element spacing d (Fig. 1). If d in the fabricated impedance tuner was less than the designed 500 μm, the largest effect would be seen at the lower frequencies of the W-band, as the electrical length of d is closer to zero and the matching becomes very sensitive to backshort positions. Indeed, delicate measurements under the microscope show that $d = 470$ μm. However, this inaccuracy only partly explains the small differences in simulations and measurements and it is assumed that some error comes from the four-port simulations of the double-T junction with HFSS. It is also possible that misalignment between the split-waveguide block halves occurred during the milling or in the assembly. However, this is very difficult to detect, especially near the double-T junction. The measured insertion loss of the waveguide impedance tuner over the W-band with two different backshort positions is shown in Fig. 7. The average insertion losses are 0.30 and 0.31 dB for the different backshort positions, respectively.

B. Repeatability of Reflection Coefficient

As discussed above, the tuning accuracy of the waveguide impedance tuner is very good even when it is tuned manually with micrometer heads. The repeatability of the impedance tuner depends on the accuracy of tuning and rigidity of the tuner structure. The latter is assumed to be excellent because the only moving parts inside the structure are the slides that the dielectric slabs are attached to. The machined slides have a very tight fit with the guide channels and can move only in wanted directions. We have studied the repeatability of the impedance tuner by measuring the same randomly chosen

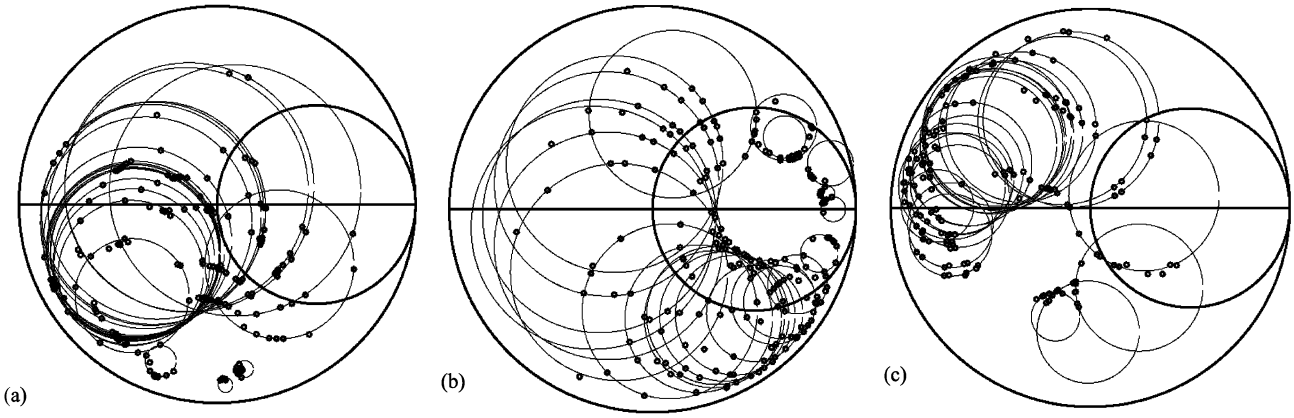

Fig. 6. Measured input impedance coverage (points) of the tuner on the Smith diagram. (a) 75 GHz. (b) 92.5 GHz. (c) 110 GHz. Large circles represent the obtainable input impedances with one of the dielectric slabs fixed in place.

TABLE II
TUNER CHARACTERISTICS AT 75, 92.5, AND 110 GHz

	75 GHz	92.5 GHz	110 GHz
Maximum reflection coefficient	0.935	0.96	0.952
Maximum VSWR	29.8	49.0	40.7
Simulated Smith diagram coverage	81 %	77 %	74 %
Measured Smith diagram coverage	70 %	76 %	71 %
Simulated combined Smith diagram coverage (Port 1 and 2)	91 %	94 %	94 %
Standard deviation in magnitude	0.0012	0.00035	0.00003
Standard deviation in phase	0.17^o	0.17^o	0.18^o

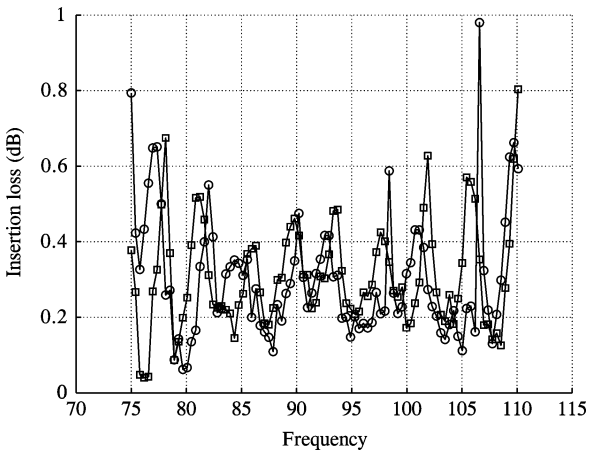

Fig. 7. Insertion loss of the waveguide impedance tuner over the W-band. The circles denote the backshort positions of 2 and 10 mm and the squares the positions 8 and 4 mm, respectively.

reflection coefficient (same backshort position) manually 30 times (only ten measurements are shown in Fig. 8 for clarity). Between measurements, the backshort positions were changed arbitrarily and then returned to original settings. The mean reflection coefficients obtained with this randomly chosen tuner position were $0.764\angle 31.06^\circ$ at 75 GHz, $0.062\angle 51.53^\circ$ at 92.5 GHz, and $0.0064\angle 77.47^\circ$ at 110 GHz. The corresponding standard deviations in the magnitude and phase of the reflection coefficient are presented in Table II. As can be seen in Fig. 8, the differences in the magnitude and phase of consecutively measured reflection coefficients are very small even when the tuner is operated manually with the micrometer heads. With the previously mentioned automated linear motors, the repeatability would be considerably better, due to the two decade improvement in positioning accuracy. The nonintuitive result, that the magnitude of the reflection coefficient is the most sensitive at 75 GHz, where the wavelength is the longest, originates from the fact that the randomly chosen reflection coefficient happens to be at the sensitive region of the Smith diagram, as can be seen in Fig. 6(a). A disadvantage of this type of impedance tuner is that the change in the impedance is different for constant steps of the slab position.

C. Scalability of Waveguide Impedance Tuner

According to the authors' knowledge, there are currently no commercial standalone impedance tuners above 170 GHz. The noise figure measurements are already being performed at W-band [3] and the need for sensitive receivers for astronomical and other applications is driving the development of noise measurements towards submillimeter wavelengths. Moreover, an accurate, large-range, and low-loss impedance tuner could be used to optimize mixers and doublers operating at submillimeter wavelengths. In one type of commercial impedance tuner [4], [5], a needle probe is moved inside a slotted waveguide. The place and depth of the probe determines the phase and magnitude of the reflection coefficient. These impedance tuners are accurate and exhibit low losses and good Smith diagram coverage at W-band and below, but as frequency increases, some problems start to arise. The smallest achievable phase step is directly proportional to the probe positioning accuracy. For example, a 10-μm tuning distance corresponds to a 1.7° phase shift at 92.5 GHz with the traditional backshorts, but only to a 0.37° phase shift in our dielectric-based backshort [14]. In our design, the phase shift is caused by the movement of the dielectric slab inside the waveguide (change in the electrical distance of the waveguide fixed short) and is, therefore, controllable by the choice of the material and dimensions of the slab. This enables even more accurate tuning, e.g., by decreasing the thickness or width of the dielectric slab. This feature is a great advantage at submillimeter wavelengths (300 GHz). At these frequencies, the fabrication of waveguide impedance tuners based on probes or traditional backshorts becomes very difficult. Suitability of different backshorts at submillimeter wavelengths is discussed in [27]. As frequency increases, the size of the waveguides decreases. For example, a WR-3 waveguide designed to operate at the frequency band

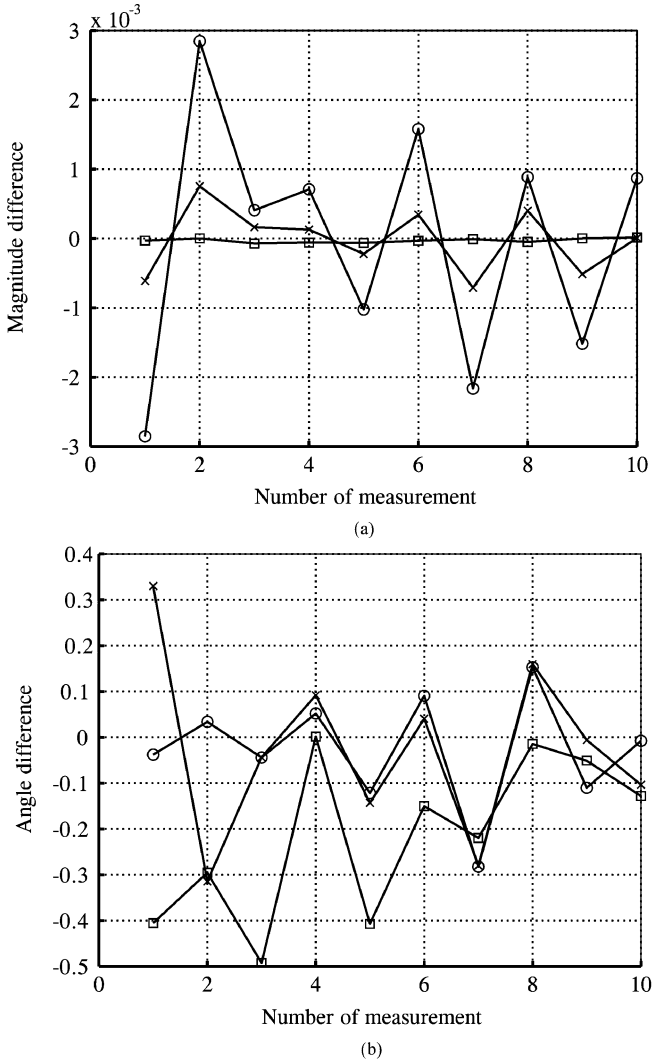

Fig. 8. Difference in the reflection coefficient between consecutive measurements of the same backshort position. (a) Magnitude. (b) Phase angle. Circles denote the frequency: 75 GHz, crosses: 92.5 GHz, and squares: 110 GHz.

of 220–325 GHz has a width of 0.86 mm. Machining a slot wide enough for the probe, but narrow enough to avoid the disturbance of the surface current in the waveguide walls and, hence, causing losses, is very demanding. The fabrication of magic-T-based impedance tuners at submillimeter wavelengths is difficult due to the complex structure and the fact that the correct alignment of the traditional contacting and noncontacting backshorts in a very small waveguide for reliable operation is very demanding. In our design, the waveguide is intact, except for the very narrow guide channel for the dielectric slab at the end of the waveguide. The fabrication techniques used in our tuner design are relatively simple. The split-waveguide block halves are milled with traditional machining techniques and the rectangular quartz slabs are fabricated with diamond cutting. These techniques are mature and split-block mixers and multipliers with quartz substrates have been demonstrated, e.g., at 220 GHz [28] and 640 GHz [29], [30]. With the state-of-the-art high precision equipment, rectangular waveguides have been directly machined up to 2.5 THz [31]. If the wanted structures cannot be fabricated using conventional machining, micromachining techniques [32]–[34] can be used instead. The metallic and dielectric losses are not of a great concern. In the rectangular waveguides, the metal losses per a wavelength are proportional to the square root of the frequency and the dielectric losses per wavelength remain constant [15, pp. 18 and 57]. The surface accuracy limits are of course more severe, but as discussed above, the conventionally machined rectangular waveguides can be well used at submillimeter wavelengths.

As a design example, a waveguide impedance tuner with WR-2 (325–500 GHz) waveguides could be realized as follows. The waveguide structure is milled using the split-waveguide block technique. The 50-μm-thick and 150-μm-wide quartz slabs are fabricated with the diamond cutting. The guide channel for the quartz slab is 254-μm wide and 70-μm high. The cutoff frequency for the waveguide TE_{10} mode is 1.1 THz in this quartz filled channel. High-precision (with the nonrotating spindle) micrometer heads with 2.5-mm tuning range and 1-μm tuning accuracy are connected to the slides in which the quartz slabs are attached. With this design, a 10-μm tuning distance corresponds to a 1.5° phase shift at 412.5 GHz, whereas with the traditional backshorts, the phase shift would be 7.0°. Preliminary simulations show that the return loss for this backshort design would be below 0.3 dB. In addition, in [14], the performance of a dielectric-based backshorts is studied at frequency bands of 140–220 and 220–325 GHz, and it is concluded that they exhibit low losses at both frequency bands and are suitable for the submillimeter wave operation. Due to the use of the dielectric-based backshorts, our waveguide impedance tuner design can be easily reproduced at submillimeter wavelengths with reliable, accurate, and low-loss operation.

V. Conclusion

A waveguide impedance tuner for W-band applications has been designed, fabricated, and measured. The impedance tuner consists of two dielectric-based backshorts forming a double-T junction with a WR-10 waveguide. Simulations and measurements show that it exhibits excellent impedance coverage, tuning accuracy, repeatability, low losses, and a high VSWR over the frequency band of 75–110 GHz. Due to the length difference in input and output waveguides, the impedance coverage can be further increased by turning the tuner around. The measured impedance coverage on the Smith diagram is more than 70% at the W-band. By turning the tuner around, the estimated impedance coverage for the fabricated tuner is over 90%. The tuner is easily scalable to submillimeter wavelengths, where, to the authors' knowledge, there are no commercial standalone impedance tuners currently available.

Acknowledgment

The authors acknowledge E. Kahra, Radio Laboratory, TKK Helsinki University of Technology, Espoo, Finland, and H. Rönnberg, Metsähovi Radio Observatory, TKK Helsinki University of Technology, for the fabrication of the impedance tuner.

References

[1] C. E. McIntosh, R. D. Pollard, and R. E. Miles, "Novel MMIC source-impedance tuners for on-wafer microwave noise-parameter measurements," *IEEE Trans. Microw. Theory Tech.*, vol. 47, no. 2, pp. 125–131, Feb. 1999.

[2] M. Kantanen, M. Lahdes, T. Vähä-Heikkilä, and J. Tuovinen, "A wideband on-wafer noise parameter measurement system at 50–75 GHz," *IEEE Trans. Microw. Theory Tech.*, vol. 51, no. 5, pp. 1489–1495, May 2003.

[3] T. Vähä-Heikkilä, M. Lahdes, M. Kantanen, and J. Tuovinen, "On-wafer noise parameter measurements at W-band," *IEEE Trans. Microw. Theory Tech.*, vol. 51, no. 6, pp. 1621–1628, Jun. 2003.
[4] R. Drury, R. D. Pollard, and C. M. Snowden, "A 75–110 GHz automated tuner with exceptional range and reliability," *IEEE Microw. Guided Wave Lett.*, vol. 6, no. 10, pp. 378–379, Oct. 1996.
[5] G. R. Simpson, R. L. Eisenhart, B. B. Szendrenyi, and R. J. Maury, "Reduced height waveguide tuner for impedance matching," U.S. Patent 5 910 754, Jun. 8, 1999.
[6] P. Krejcik, "Waveguide stub-line tuning of RF cavities with heavy beam loading," in *Proc. Particle Accelerator Conf.*, 1997, pp. 3030–3032.
[7] M. A. Rothman, "A calibrated tuner for millimeter device evaluation," in *Proc. Energy Inform. Technol. in Southeast*, 1989, pp. 163–167.
[8] H. Xu, C. H. Smith, J. L. Hesler, B. S. Deaver, and R. M. Weikle II, "A non-contacting tunable waveguide backshort for terahertz applications," in *IEEE MTT-S Int. Microw. Symp. Dig.*, 2006, pp. 1919–1922.
[9] J. Papapolymerou, K. L. Lange, C. L. Goldsmith, A. Malczewski, and J. Kleber, "Reconfigurable double-stub tuners using MEMS switches for intelligent RF front-ends," *IEEE Trans. Microw. Theory Tech.*, vol. 51, no. 1, pp. 271–278, Jan. 2003.
[10] T. Vähä-Heikkilä, J. Varis, J. Tuovinen, and G. M. Rebeiz, "W-band RF MEMS double and triple-stub impedance tuners," in *IEEE MTT-S Int. Microw. Symp. Dig.*, 2005, pp. 923–926.
[11] Y. Lu, L. P. B. Katehi, and D. Peroulis, "High-power MEMS varactors and impedance tuners for millimeter-wave applications," *IEEE Trans. Microw. Theory Tech.*, vol. 53, no. 11, pp. 3672–3678, Nov. 2005.
[12] V. M. Lubecke, W. R. McGrath, P. A. Stimson, and D. B. Rutledge, "Micromechanical tuning element in a 620-GHz monolithic integrated circuit," *IEEE Trans. Microw. Theory Tech.*, vol. 46, no. 12, pp. 2098–2103, Dec. 2006.
[13] V. S. Möttönen, P. Piironen, and A. V. Räisänen, "Novel tunable waveguide backshort for millimeter and submillimeter wavelengths," *IEEE Microw. Wireless Compon. Lett.*, vol. 11, no. 9, pp. 370–372, Sep. 2001.
[14] V. S. Möttönen and A. V. Räisänen, "Design of a dielectric-based tunable waveguide backshort," in *Proc. 35th Eur. Microwave Conf.*, 2005, pp. 589–592.
[15] N. Marcuvitz, *Waveguide Handbook*. London, U.K.: Peregrinus, 1986.
[16] R. E. Collin, *Foundations for Microwave Engineering*. New York: McCraw-Hill, 1992.
[17] R. L. Eisenhart and R. C. Monzello, "A better waveguide short circuit," in *IEEE MTT-S Int. Microw. Symp. Dig.*, 1982, pp. 360–362.
[18] W. R. McGrath, "Noncontacting waveguide backshort," U.S. Patent 5 138 289, Aug. 11, 1992.
[19] M. K. Brewer and A. V. Räisänen, "Dual-harmonic noncontacting millimeter waveguide backshorts: Theory, design and test," *IEEE Trans. Microw. Theory Tech.*, vol. MTT-30, no. 5, pp. 708–714, May 1982.
[20] R. A. Linke and M. V. Schneider, "Millimeter waveguide shorts," U.S. Patent 4216450, Aug. 5, 1980.
[21] "Sliding short eases measurements," *Microwaves*, vol. 9, no. 12, Dec. 1970, (anonymous authorship).
[22] A. R. Kerr, "An adjustable short-circuit for millimeter waveguides," Nat. Radio Astron. Observatory, Electron. Div. Internal Rep. 280, 1988, 26 pp.
[23] W. R. McGrath, T. M. Weller, and L. P. B. Katehi, "A novel noncontacting waveguide backshort for submillimeter wave frequencies," *Int. J. Infrared Millim. Waves*, vol. 16, no. 1, pp. 237–256, Jan. 1995.
[24] T. M. Weller, L. P. B. Katehi, and W. R. McGrath, "Analysis and design of a novel noncontacting waveguide backshort," *IEEE Trans. Microw. Theory Tech.*, vol. 43, no. 5, pp. 1023–1030, May 1995.
[25] B. N. Ellison, L. T. Little, C. M. Mann, and D. N. Matheson, "Quality and performance of tunable waveguide backshorts," *Electron. Lett.*, vol. 27, no. 2, pp. 139–141, Jan. 1991.
[26] T. Newman and K. T. Ng, "Planar noncontacting short circuits for millimeter-wave and submillimeter-wave applications," *IEEE Microw. Guided Wave Lett.*, vol. 2, no. 10, pp. 412–414, Oct. 1992.
[27] V. S. Möttönen, "Receiver front-end circuits and components for millimetre and submillimeter wavelengths," Doctor Sci. Technol. thesis, Radio Lab., Helsinki Univ. Technol., Espoo, Finland, 2005, Rep. S 269.
[28] A. V. Räisänen, D. Choudhury, R. J. Dengler, J. E. Oswald, and P. H. Siegel, "A novel split-waveguide mount design for millimeter- and submillimeter-wave frequency multipliers and mixers," *IEEE Microw. Guided Wave Lett.*, vol. 3, no. 10, pp. 369–371, Oct. 1993.
[29] P. H. Siegel, I. Mehdi, R. J. Dengler, T. H. Lee, D. A. Humphrey, and A. Pease, "A 640 GHz planar-diode fundamental mixer/receiver," in *IEEE MTT-S Int. Microw. Symp. Dig.*, 1998, pp. 407–410.
[30] I. Mehdi, P. H. Siegel, A. Humphrey, R. J. Dengler, T. H. Lee, J. E. Oswald, D. A. Pease, R. Lin, H. Eisele, R. Zimmermann, and N. Erickson, "An all solid-state 640 GHz subharmonic mixer," in *IEEE MTT-S Int. Microw. Symp. Dig.*, 1998, pp. 403–406.
[31] P. H. Siegel, R. P. Smith, and M. C. Gaidis, "2.5-THz GaAs monolithic membrane-diode mixer," *IEEE Trans. Microw. Theory Tech.*, vol. 47, no. 5, pp. 596–604, May 1999.
[32] C. M. Mann, "Fabrication technologies for terahertz waveguide," in *Proc. Terahertz Electron.*, 1998, pp. 46–49.
[33] P. L. Kirby, D. Pukala, H. Manohara, I. Mehdi, and J. Papapolymerou, "Characterization of micromachined silicon rectangular waveguide at 400 GHz," *IEEE Microw. Wireless Compon. Lett.*, vol. 16, no. 6, pp. 366–368, Jun. 2006.
[34] V. M. Lubecke, K. Mizuno, and G. M. Rebeiz, "Micromachining for terahertz applications," *IEEE Trans. Microw. Theory Tech.*, vol. MTT-46, no. 11, pp. 1821–1831, Nov. 1998.

Tero Kiuru (S'06) was born in Tampere, Finland, on June 11, 1980. He received the M.Sc. degree in electrical engineering from the TKK Helsinki University of Technology, Espoo, Finland, in 2006, and is currently working toward the Ph.D. degree at the TKK Helsinki University of Technology.

Since 2003, he has been a Research Assistant and Researcher with the Radio Laboratory, TKK Helsinki University of Technology. He is a member of the TKK Graduate School of Electrical and Communications Engineering. His current research interests include millimeter- and submillimeter-wave sources, characterization and modeling of Schottky diodes, and on-wafer measurement and calibration methods.

Ville S. Möttönen (S'00–M'05) was born in Oulu, Finland, in 1972. He received the Master of Science (Tech.), Licentiate of Science (Tech.), and Doctor of Science (Tech.) degrees in electrical engineering from the TKK Helsinki University of Technology, Espoo, Finland, in 1996, 1999, and 2005, respectively.

From 1996 to 2007, he was with the Radio Laboratory (and its Millimeter Wave Group), TKK Helsinki University of Technology, as a Research Assistant and Research Associate. He is currently with the National Board of Patents and Registration of Finland, Helsinki, Finland. His current research interests include antennas for mobile devices and the development and design of millimeter- and submillimeter-wave receivers.

Antti V. Räisänen (S'76–M'81–SM'85–F'94) received the D.Sc degree (Tech.) in electrical engineering from the TKK Helsinki University of Technology, Espoo, Finland, in 1981.

In 1989, he became the Professor Chair of Radio Engineering with TKK Helsinki University of Technology. In 1997, he became the Vice-Rector of TKK Helsinki University of Technology (1997–2000). He has been a Visiting Scientist and Professor with the University of Massachusetts, Amherst, Chalmers University of Technology, Göteborg, Sweden, University of California at Berkeley, California Institute of Technology, Jet Propulsion Laboratory (JPL), Pasadena, and Paris Observatory, Paris, France, and the University of Paris 6, Paris, France. He currently supervises research in millimeter-wave components, antennas, receivers, microwave measurements, etc. with the TKK Radio Laboratory and Millimetre Wave Laboratory of Finland—ESA External Laboratory (MilliLab). He leads The Centre of Smart Radios and Wireless Research (SMARAD), which has obtained the national status of Centre of Excellence (CoE) in Research for 2002–2007 and 2008–2013. He has authored or coauthored approximately 400 scientific papers and six books, including *Radio Engineering for Wireless Communication and Sensor Applications* (Artech House, 2003).

Dr. Räisänen has been conference chairman for four international microwave and millimeter wave conferences. He was an associate editor for the IEEE TRANSACTIONS ON MICROWAVE THEORY AND TECHNIQUES (2002–2005). In 2006, he became a member of the Board of Directors of the European Microwave Association (EuMA).